

Raman study and lattice dynamics of single molecular layers of MoS₂

S. Jiménez Sandoval,* D. Yang, R. F. Frindt, and J. C. Irwin

Department of Physics, Simon Fraser University, Burnaby, British Columbia, Canada V5A 1S6

(Received 8 April 1991)

A valence-force-field model has been used to study the lattice dynamics of molybdenum disulfide single molecular layers. A comparison between the room-temperature Raman spectra of aqueous suspensions and the calculated phonon-dispersion curves for single layers of MoS₂ with trigonal prism and octahedral coordination indicates that MoS₂ single layers adopt a structure in which the Mo atoms are octahedrally coordinated, as opposed to bulk MoS₂ where the trigonal prism coordination is usually found. Besides the zone-center modes, strong Raman peaks have been observed at 156, 226, and 333 cm⁻¹. The presence of these peaks is attributed to a zone-folding mechanism resulting from the formation of a $2a_0 \times a_0$ superlattice in the single layers of MoS₂. The superlattice is, in turn, believed to correspond to the basal-plane atomic arrangement of a distorted octahedral structure. Lattice-dynamics calculations based on an octahedrally coordinated structure with a significant metal-metal interaction yield good agreement with the observed frequencies. When the single molecular layers restack and the sulfur-sulfur interaction between the layers is recovered, the layers convert back to the trigonal prismatic configuration of crystalline MoS₂.

I. INTRODUCTION

Single molecular layers of molybdenum disulfide in aqueous suspension have been obtained by exfoliating lithium-intercalated MoS₂ powder.¹ X-ray diffraction and preliminary Raman results indicated² that the MoS₂ single layers underwent a structural phase transition from the trigonal prism coordination of the bulk material to a structure in which the molybdenum atoms are octahedrally coordinated. Moreover, evidence of a crystalline lattice distortion that produced a $2a_0$ superlattice was also found in the x-ray diffraction patterns obtained from the single layers. In order to gain further insight into the structure of single-layer MoS₂, a detailed Raman scattering study of the MoS₂ single molecular layers in aqueous suspension has been performed. Raman spectroscopy is a useful technique to study crystallographic phase transitions because of its sensitivity to variations of the lattice symmetry. In addition, thin films obtained by restacking the single molecular layers on glass substrates were also studied by this technique.

The lattice dynamics of bulk $2H$ -MoS₂ have been studied rather extensively both experimentally and theoretically. The experimental studies in bulk samples include Raman scattering³⁻⁸ and infrared^{8,9} experiments as well as inelastic neutron scattering investigations.¹⁰ In an early calculation, Bromley¹¹ used a simple one-layer lattice dynamics model that considered elastic nearest-neighbor interactions in the Born-von Kármán formalism. Bromley's method yielded analytical expressions that were in good agreement with the experimental results for the zone-center modes. Wieting and Verble¹² used a linear-chain model to analyze the effects of interlayer coupling on the lattice dynamics of various transition-metal dichalcogenides including $2H$ -MoS₂. A more sophisticated lattice dynamics model was developed by

Wakabayashi, Smith, and Nicklow¹⁰ to fit their neutron-scattering data and thus obtain the phonon dispersion curves of $2H$ -MoS₂. Their approach combined an axially symmetric model, to account for the weak Van der Waals-type interlayer interaction, with a valence force field model, which is suitable for describing the strong covalent nature of the interlayer interactions.

In this paper a valence force field model due to Wakabayashi, Smith, and Nicklow¹⁰ has been used to calculate the phonon dispersion curves of single molecular layers of MoS₂ for the case of trigonal prismatic coordination, hereafter designated as τ -MoS₂, and for single molecular layers in which the Mo atoms are octahedrally coordinated, hereafter designated as Ω -MoS₂. For bulk crystals, the standard notation ($2H$) will be employed. The calculated frequencies of the zone-center ($q=0$) vibrations allow a direct comparison with the first-order Raman peaks that are expected for the two different structures. In addition, the calculated phonon dispersion curves enable one to predict additional phonons that would be observed given the existence of a superlattice structure in the single layers. The formation of a superlattice leads to a folding of normally Raman inactive zone-boundary modes into the center of the zone.¹³ From a direct comparison of the Raman spectra with the calculated dispersion curves, we have found that our experimental results are consistent with the formation of a superlattice in octahedrally coordinated single layers of MoS₂, if a strong metal-metal interaction is added to our model. This in turn implies that the single layers have a distorted octahedral structure.

II. EXPERIMENT

A detailed description of the method used for the preparation of single molecular layers of MoS₂ has been

published previously.^{1,14} Briefly, MoS₂ is intercalated with lithium to form Li_xMoS₂ with $x \approx 1.0$ and the intercalated samples are exfoliated by immersion in distilled water. The MoS₂ layers are separated from the Li by-products by rinsing in water and centrifuging three or four times. An aqueous suspension of the MoS₂ layers is obtained by adding water to the desired concentration.

Thin films of the restacked MoS₂ layers were produced by a spreading technique¹⁴ which yielded films with thicknesses varying between 35 and 200 nm. The films were produced using freshly prepared suspensions and were then allowed to stand in air over a period of a few months and their properties monitored at different times during this interval.

The Raman-scattering spectra were obtained by exciting the samples with the 488.0- or 514.5-nm lines of an argon-ion laser at room temperature. To minimize laser heating effects, the beam was focused on the samples with the aid of a cylindrical lens. Typical incident laser powers were of the order of 10 W/cm². The scattered light was then collected in a near backscattering configuration and concentrated at the entrance slit of a computer-controlled triple spectrometer. An ITT Mep-sicon imaging detector was used to analyze the signal and the data were stored and processed in an IBM/PC microcomputer.

The Raman spectra of the MoS₂ aqueous suspension were obtained in a container-free fashion by drilling a tapered 1.7-mm diameter pinhole in a copper plate and filling this hole with the MoS₂ suspension, the suspension being held in place by surface tension. The Raman spectra of the single layers obtained in this way, were free from spurious signals such as scattering from glass covering plates. A small amount of scattering from air was present at frequencies below the present range of interest. Raman spectra were also obtained from restacked films on a glass substrate both with the films in air and mounted in an evacuated Displex refrigerator.

III. RESULTS AND ANALYSIS

A. Group theory analysis

Figure 1 illustrates the trigonal prism (a) and octahedral coordinations (b) for MoS₂. The octahedral coordination can be obtained from the trigonal prism structure

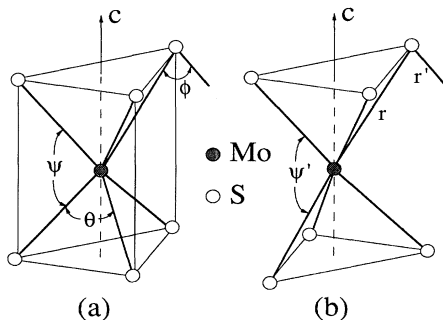


FIG. 1. Schematic diagram of the structure of MoS₂ with (a) trigonal prism and (b) octahedral coordination.

by rotating one of the sulfur basal planes by 60° around the *c* axis. Clearly, these structures have different symmetry elements. The crystalline structure of 2*H*-MoS₂ belongs to the D_{6h}^4 ($P6_3/mmc$) space group. Its unit cell is composed of two Mo atoms occupying sites with point-group symmetry D_{3h} and four sulfur atoms in sites with point-group symmetry C_{3v} . A correlation of the site symmetries with the factor group D_{6h} allows one to associate the 18 normal modes of vibration at $q=0$ with the following irreducible representations:³

$$\Gamma \equiv A_{1g} \otimes 2A_{2u} \otimes 2B_{2g} \otimes B_{1u} \otimes E_{1g} \otimes 2E_{1u} \otimes 2E_{2g} \otimes E_{2u} ,$$

where A_{2u} and E_{1u} correspond to translational acoustic modes, and where A_{1g} , E_{1g} , and E_{2g} are Raman active. The frequencies of the 2*H*-MoS₂ Raman modes determined experimentally are the following:⁸

$$\begin{aligned} \omega(E_{2g}^2) &= 32 \text{ cm}^{-1}, & \omega(E_{1g}) &= 287 \text{ cm}^{-1}, \\ \omega(E_{2g}^1) &= 383 \text{ cm}^{-1}, & \omega(A_{1g}) &= 409 \text{ cm}^{-1}. \end{aligned} \quad (1)$$

The low-frequency E_{2g}^2 mode corresponds to the interlayer interaction with rigid layer motion and the remaining three modes correspond to intralayer vibration.^{6,8}

The frequencies of the intralayer vibrational modes in 2*H*-MoS₂ are expected to be essentially the same as those of a single layer. Wieting and Verble^{3,4,12} pointed out that in layered structures, such as MoS₂, the weak interlayer interaction couples the intralayer vibrations in the two layers of the unit cell. "In phase" coupling between the layers gives rise to the infrared active modes and "out of phase," to the Raman active modes. The Raman and the infrared modes in a given conjugate pair thus have frequencies that are almost identical because of the relatively small interlayer coupling. More generally, the stacking sequence of the layers of MoS₂ will have almost no effect on the frequencies of the observed modes, but will change the symmetry and hence the selection rules governing their optical activity.

The factor group describing the symmetry of a single MoS₂ layer with trigonal prismatic coordination (τ -MoS₂) is D_{3h} with three atoms in the unit cell.¹¹ There are thus nine phonons at the zone center (Γ) and their symmetries can be represented by the irreducible representations of D_{3h} as

$$\Gamma \equiv 2A_2'' \otimes A_1' \otimes 2E' \otimes E'' .$$

In this case, the acoustic modes are represented by $A_2'' \otimes E'$, one A_2'' mode is infrared active, A_1' and E'' are Raman active, and one E' mode is both Raman and infrared active. A correlation with the D_{6h} point group allows one to associate E' with the 383-cm⁻¹ Raman mode and 384-cm⁻¹ infrared mode of 2*H*-MoS₂, E'' with E_{1g} and A_1' with A_{1g} .

The symmetry of the 1*T* structure is described by the space group D_{3d}^3 ($P\bar{3}m1$) with three atoms in the unit cell.¹² The factor group describing the symmetry of an octahedral single layer (Ω -MoS₂) is D_{3d} with the metallic atoms located in sites with symmetry D_{3d} and the chalcogen atoms occupying sites with C_{3v} symmetry. The

correlation of site symmetries with the group D_{3d} yields the following irreducible representations for the phonons at the zone center:

$$\Gamma \equiv A_{1g} \otimes 2A_{2u} \otimes E_g \otimes 2E_u .$$

The acoustic modes are represented in this case by $A_{2u} \otimes E_u$ while the remaining A_{2u} and E_u modes are infrared active and only the A_{1g} and E_g modes are Raman active. From a group-theoretical correlation, one finds that the A_{1g} and E_g modes of Ω -MoS₂ should have frequencies almost equal to those of the A_{1g} and E_{1g} modes of bulk $2H$ -MoS₂. This assertion is confirmed by the lattice-dynamics calculations described in the following section.

B. MoS₂ single-layer phonon dispersion curves

A valence-force-field (VFF) model has been employed to calculate the phonon dispersion curves of single molecular layers of MoS₂ with trigonal prism and octahedral coordinations. In the ideal structures considered here, the height of the prisms is equal to the hexagonal lattice parameter a_0 , which for bulk MoS₂ is 3.16 Å, with the metal atom situated at the center, Fig. 1. The Mo-S distance is equal to $(\frac{7}{12})^{1/2}a_0$ for both structures. The basal-plane projection of the Brillouin zone is a hexagon¹¹ (Fig. 2), whose orientation and dimensions are the same for all of the $2H$ -MoS₂, τ -MoS₂, and Ω -MoS₂ structures.

The lattice-dynamics calculation has been carried out with the intralayer potential energy used by Wakabayashi, Smith, and Nicklow¹⁰ in modeling their neutron data for $2H$ -MoS₂. In terms of the force constants K_r , K_θ , K_ϕ , K_ψ , and $K_{r\phi}$, this potential energy is written as¹⁰

$$U = \frac{1}{2}K_r(\Delta r)^2 + \frac{1}{2}K_\theta(r_0 \Delta\theta)^2 + \frac{1}{2}K_\phi(r_0 \Delta\phi)^2 + \frac{1}{2}K_\psi(r_0 \Delta\psi)^2 + \frac{1}{2}K_{r\phi} \Delta r \Delta r' , \quad (2)$$

where r_0 is the equilibrium Mo—S bond length and r , r' , θ , ϕ , and ψ are defined in a manner identical to that of

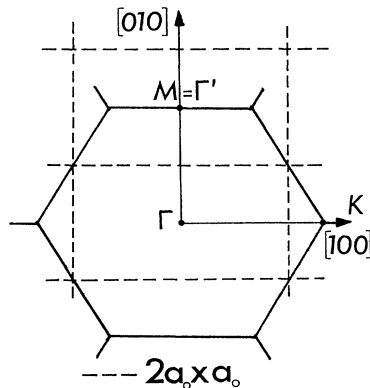


FIG. 2. Reciprocal space diagram illustrating the relationship between the basal plane projection of the Brillouin zone of $2H$ -MoS₂ (solid lines) and the two-dimensional Brillouin zone of a $2a_0 \times a_0$ superlattice.

TABLE I. Force constants used to calculate the phonon dispersion curves for single molecular layers of MoS₂, (10^5 dyn/cm). The values shown were obtained from Ref. 10 and are in units of 10^5 dyn/cm.

K_r	1.3846
K_θ	0.1502
K_ψ	0.1381
K_ϕ	0.1892
$K_{r\phi}$	-0.1722

Ref. 10, and are shown in Fig. 1. Using the force-constant values given in Table I (and two interlayer constants which are not of interest here), Wakabayashi, Smith, and Nicklow¹⁰ obtained good agreement with the measured phonon dispersion curves of $2H$ -MoS₂.

The phonon dispersion curves for both τ -MoS₂ and Ω -MoS₂ have been calculated using Eq. (2) and the force constants given in Table I. In doing so, it is assumed that Ω -MoS₂ is obtained from τ -MoS₂ by a simple 60° rotation of one of the sulfur planes and thus the equilibrium values of r , ϕ , and θ are the same for both structures. The angles ψ and ψ' (Fig. 1) are different, but as a first approximation, it is assumed that K_ψ and $K_{\psi'}$ are equal. It has also been assumed that surface modes do not play an important role in the lattice dynamics of MoS₂ single layers. This appears justified because of the inert nature of the layer surfaces which is manifested by the weak binding energy between adjacent layers in bulk crystals.

The calculated phonon dispersion curves of an infinite MoS₂ single layer along the [010] and [100] directions of the hexagonal two-dimensional Brillouin zone are shown for τ -MoS₂ in Fig. 3, and for Ω -MoS₂ in Fig. 4. Table II lists the calculated frequencies of the vibrational modes

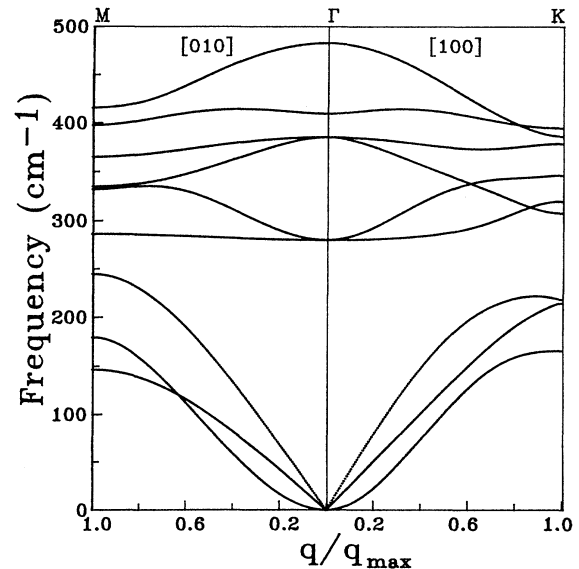


FIG. 3. Calculated phonon dispersion curves along the [010] and [100] directions of single molecular layers of MoS₂ with trigonal prism (τ -MoS₂) coordination.

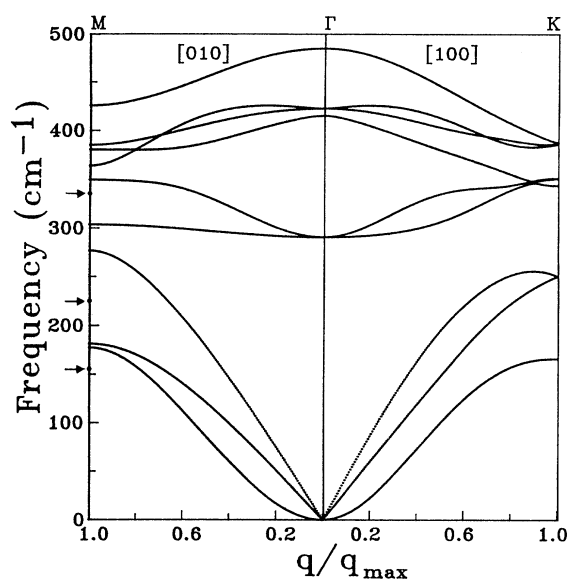


FIG. 4. Calculated phonon dispersion curves along the [010] and [100] directions of single molecular layers of MoS₂ with octahedral (Ω -MoS₂) coordination. The small arrows indicate the frequencies of the J_1 , J_2 , and J_3 features in the Raman spectra of Fig. 5.

at Γ for both structures. The symmetry of each mode has been assigned by considering the symmetry of the dynamical matrix eigenvectors. By comparing the frequencies given in Eq. (1) with those in Table II, it can be noticed that the $q=0$ intralayer modes of τ -MoS₂ have almost the same frequency as those in $2H$ -MoS₂ and that the frequencies of the Raman modes E_g and A_{1g} of Ω -MoS₂ should be nearly the same as those of the E_{1g} and A_{1g} modes of $2H$ -MoS₂. One important difference, however, is that the strong 383-cm^{-1} Raman peak^{6,8} of $2H$ -MoS₂, must be absent (Table II) in the case of octahedrally coordinated MoS₂, a result that is in agreement with the symmetry considerations of the previous section.

C. Raman spectra of single layer suspensions

Figure 5(a) shows a typical room-temperature Raman spectrum obtained from a freshly prepared MoS₂ single layer aqueous suspension. It is clear from this figure that there are two relatively strong features at 287 cm^{-1} and

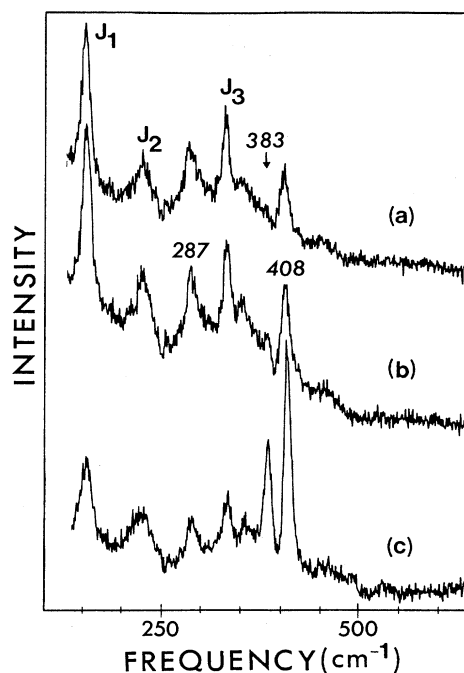


FIG. 5. Room-temperature Raman spectra of (a) a freshly prepared MoS₂ single layer aqueous suspension, (b) a 12-day-old suspension, and (c) a 1.5-month-old suspension.

408 cm^{-1} . Furthermore, Fig. 5(a) does not contain any evidence of a spectral peak near 383 cm^{-1} . In spectra obtained from $2H$ -MoS₂ the 383-cm^{-1} is usually observed^{6,8} to have an intensity that is more than an order of magnitude greater than that of the E_g mode at 287 cm^{-1} [cf. Fig. 6(c)] and one would expect a similar ratio in spectra obtained from τ -MoS₂. The presence of the two peaks at 287 cm^{-1} and 408 cm^{-1} in Fig. 5(a), in conjunction with the absence of a peak at 383 cm^{-1} thus leads one directly to the conclusion that in freshly prepared aqueous suspensions the single layers of MoS₂ are octahedrally coordinated, in agreement with previous results.² It is also clear from Table II that the peaks at 287 and 408 cm^{-1} can be identified as the E_g and A_{1g} modes of Ω -MoS₂.

The additional peaks at 156 cm^{-1} (J_1), 226 cm^{-1} (J_2), and 333 cm^{-1} (J_3) which appear in the spectra of Fig. 5, are not normally seen in the Raman spectrum of $2H$ -

TABLE II. Calculated frequencies of the vibrational modes at Γ ($q=0$) for single molecular layers of MoS₂ with undistorted trigonal prism and octahedral coordinations.

Mode	Trigonal prism (τ -MoS ₂)				Octahedral (Ω -MoS ₂)			
	E''	E'	A'_1	A''_2	E_g	A_{1g}	E_u	A_{2u}
Activity	R	R,IR	R	IR	R	R	IR	IR
Calculated frequency (cm ⁻¹)	280	384	407	481	290	413	421	483

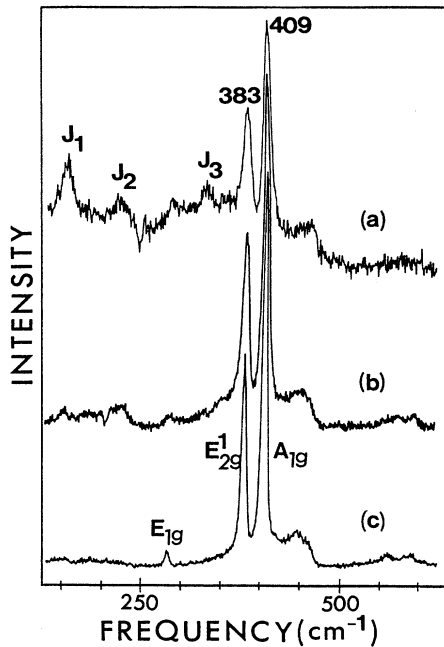


FIG. 6. Room-temperature Raman spectra of (a) a fresh restacked MoS₂ film, (b) a 2-month-old film, and (c) 2H-MoS₂ powder before exfoliation.

MoS₂ crystals^{6,8} [Fig. 6(c)]. The second-order Raman spectrum of 2H-MoS₂ has been studied by Chen and Wang.⁶ They found two second-order peaks at 150 cm⁻¹ and 188 cm⁻¹ in the low frequency (< 400 cm⁻¹) portion of the spectrum with an intensity that was about $\frac{1}{20}$ of the A_{1g} mode at 408 cm⁻¹. The J₁, J₂, and J₃ peaks thus have quite different frequencies and a much larger relative intensity than the two phonon features observed in 2H-MoS₂. Furthermore, Chen and Huang⁶ also observed that both of the second-order peaks at 150 and 188 cm⁻¹ were absent in spectra taken at 77 K. On the other hand, the relative intensities of peaks J₁, J₂, and J₃ obtained from fresh films at 80 K were essentially equal to those observed in spectra obtained at room temperature [Fig. 6(a)]. We can thus conclude that J₁, J₂, and J₃ do not arise from two-phonon scattering, and furthermore, attempts to correlate these features with the Raman spectra of possible contaminants such as water, hexene, LiOH, or *n*-butyllithium were not successful.

The appearance of the additional peaks J₁, J₂, and J₃, however, can be explained in terms of the existence of a superlattice, as suggested by the results of x-ray diffraction studies.² Because of wave-vector conservation, Raman spectra normally contain peaks corresponding to zone-center modes only, but if a superlattice is formed, the Brillouin zone is reduced and zone-boundary points of the original system can be brought into coincidence with Γ' of the additional zone.¹³ Raman scattering events may then involve zone-edge phonons without violating wave-vector conservation. The nature of the superlattice determines the particular point of the Brillouin-zone boundary that will be folded into the zone

center and hence determines the phonons that will be observed. X-ray diffraction patterns obtained from single layers of MoS₂ were found to be consistent with the formation of a 2a₀ × a₀ or 2a₀ × 2a₀ superlattice of the hexagonal Mo lattice.² More definitive evidence of a 2a₀ × a₀ superlattice has been obtained recently from scanning tunneling microscope images.¹⁵ For a 2a₀ × a₀ superlattice one would thus expect that the M point of the original Brillouin zone should coincide with the Γ' point of the reduced zone (Fig. 2) and that the J₁, J₂, and J₃ peaks of Fig. 5 correspond to frequencies at the M point of Ω -MoS₂.

The zone-boundary frequencies at the points M and K are tabulated in Table III for Ω -MoS₂ and the frequencies of J₁, J₂, and J₃ are also listed for comparison purposes. As is evident from this table (and from Figs. 3 and 4), the M-point frequencies for Ω -MoS₂ are in qualitative agreement with the measured values, although the calculated frequencies at the K points are in somewhat better correspondence with experiment. To make this comparison more meaningful, one must recognize that the force constants should be modified to reflect the structural differences ($\psi \neq \psi'$) between τ -MoS₂ and Ω -MoS₂ and those that might result from the formation of a superlattice. If it is assumed that the Mo-S separation remains constant^{16,17} the formation of a superlattice would result in changes in θ , ψ , and ϕ and hence K _{ψ} , K _{θ} , and K _{ϕ} should be altered. One finds however that variation of these parameters does not result in any significant improvement of the agreement with the experimental frequencies.

It is quite possible that the single layers of Ω -MoS₂ adopt a distorted octahedral structure¹⁸ similar to that of WTe₂. This possibility is suggested by the fact that the basal plane projection of the WTe₂ structure corresponds closely to a 2a₀ × a₀ superlattice of an ideal two-dimensional hexagonal lattice. Furthermore, distorted structures such as WTe₂, result from an enhanced metal-

TABLE III. Calculated frequencies at the M and K points of the Brillouin zone for octahedrally coordinated Ω -MoS₂ (undistorted) and *m* Ω -MoS₂ (distorted). The experimental frequencies of peaks J₁, J₂, and J₃ for single layer MoS₂ are also shown for comparison.

	Calculated (cm ⁻¹)			
	Ω -MoS ₂	K	M	<i>m</i> Ω -MoS ₂
M				
	175	164	155	146
	179	248	229	210
	274	342	297	336
	303	349	340	340
	348	385	359	378
	363	387	369	384
	378		379	
	384		415	
	424			
		Experimental (cm ⁻¹)		
J ₁		J ₂		J ₃
156		226		333

metal interaction^{17,18} which leads to a semimetallic, rather than semiconducting behavior. The latter aspect is consistent with the observed differences between the optical absorption spectrum of $2H$ - MoS_2 and that of single layer suspensions.¹⁶

To explore this possibility we have incorporated an additional force constant K_m in our model to represent the Mo-Mo interaction. Feldman¹⁹ has shown previously that the dominant effect resulting from the inclusion of such a force constant is a flattening of the acoustic-phonon branches. Using a value of $K_m = -0.173$ (10^5) dyn/cm we have obtained the phonon dispersion curves shown in Fig. 7. (This structural variant will be designated $m\Omega$ - MoS_2 .) The M -point frequencies are listed in Table III under $m\Omega$ - MoS_2 and it is clear that the agreement with the measured frequencies for J_1 , J_2 , and J_3 is much improved. This result thus indicates that the single layers of MoS_2 adopt a distorted octahedral coordination.

D. Phonon density of states

It is possible that the lateral dimensions of some of the MoS_2 single-layer crystallites are quite small, for example, of the order of 100 Å or less. It is known²⁰⁻²³ that as the crystal size becomes smaller, the coherence or correlation length for a phonon is reduced and the crystal momentum selection rules for Raman scattering break down. As a result phonons from an extended region of the Brillouin zone can participate in first-order scattering. When the crystallite dimensions are decreased below 100 Å the Raman lines become broadened^{21,22} if there is significant dispersion near the zone center. As the crys-

tallite sizes become even smaller ($\lesssim 20$ Å) scattering from throughout the Brillouin zone becomes allowed²⁰⁻²² and for an amorphous solid the spectrum essentially represents the density of states. In the extreme limit of very small crystallites consisting of a few atoms the concept of a phonon density of states is no longer meaningful and the Raman spectra should again yield narrow peaks corresponding to the Raman active modes of the free molecule.^{24,25} The frequencies of such modes have been found to be similar to those of the bulk crystal. Experimentally, Nemanich and Solin²⁶ have previously studied the effect of small crystallite size on the Raman spectra of graphite and correlated extra peaks in their spectra with features in the calculated phonon density of states.

For comparison with the Raman spectra obtained here we have calculated the phonon density of states corresponding to the dispersion curves of the $m\Omega$ - MoS_2 structure. Phonon frequencies were calculated at 34 842 points regularly distributed over $\frac{1}{12}$ of the two-dimensional Brillouin zone. The number of modes in a given frequency interval (1 cm^{-1}) were then simply counted and the results are displayed in Fig. 8. Our calculation was carried out using a very fine grid and thus interpolation methods²⁷ were not considered necessary to obtain a reasonably accurate picture of the density of states.

From an examination of Fig. 8 it is evident that the J_1 , J_2 , and J_3 peaks cannot be correlated with the pronounced peaks in the calculated density of states. It thus appears that the presence of J_1 , J_2 , and J_3 cannot be attributed to a breakdown in the Raman selection rules, again indicating that the M point of the Brillouin zone is selected by the formation of a superlattice in the single layers of Ω - MoS_2 . The observed broadening and shape of

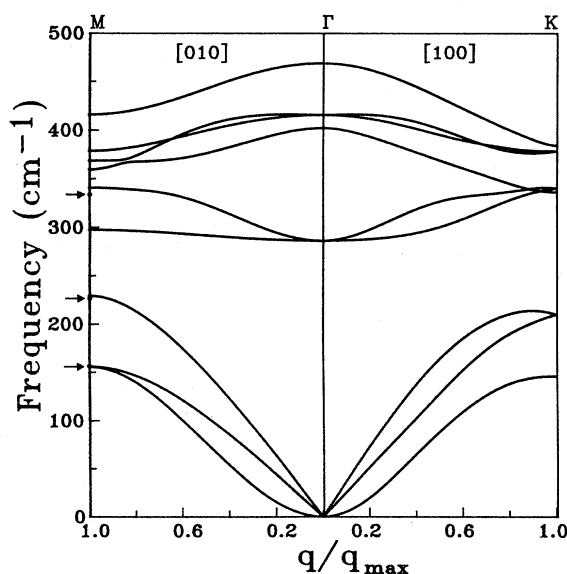


FIG. 7. Calculated phonon dispersion curves for single layers of MoS_2 with octahedral coordination and a metal-metal interaction ($m\Omega$ - MoS_2). The small arrows indicate the frequencies of the J_1 , J_2 , and J_3 features observed in the Raman spectra of Fig. 5.

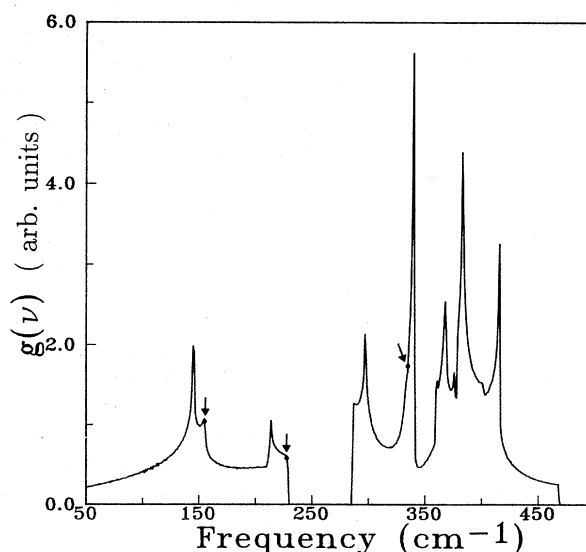


FIG. 8. Calculated phonon density of states for $m\Omega$ - MoS_2 . The small arrows indicate the frequencies of the J_1 , J_2 , and J_3 features observed in the Raman spectra of Fig. 5.

the J_2 , J_3 , and 278-cm^{-1} peaks are then quite consistent^{21,22} with the noticeable dispersion of the phonon branches near these points if the crystallite size is assumed to be about 50 \AA . The J_1 peak and the A_{1g} peak at 408 cm^{-1} are on the other hand quite symmetric which is consistent agreement with the flatness of the dispersion curves near these frequencies.

E. Effects of aging

Raman spectra were also obtained from the MoS_2 suspensions which had been allowed to age in a sealed container for days and weeks after preparation. These spectra differed significantly and systematically from those obtained from the freshly prepared suspensions. For example, Figs. 5(b) and 5(c) show the Raman spectra of a 12-day-old suspension and a 1.5-month-old suspension, respectively. As is evident from these figures, the superlattice-related peaks become weaker and the peak at 383 cm^{-1} reappears and becomes stronger as the suspension ages. This behavior can be explained by the tendency of the single layers to restack and transform back to the more stable trigonal prism coordination of bulk MoS_2 .

This transformation is more noticeable when the single molecular layers are restacked on glass substrates to form a thin film.¹³ Figure 6 shows the Raman spectra of a fresh restacked film (a), a 2-month-old film (b) and $2H\text{-MoS}_2$ powder (c). The similarity between the Raman spectrum of the 1.5-month-old suspension, Fig. 5(c), and the spectrum of the freshly prepared film, Fig. 6(a), suggests that restacking of the layers, concurrent with water removal, is the primary driving mechanism related to restoring the trigonal prism coordination. In the restacked films, this conversion may be faster because of the accelerated water evaporation that occurs when the films are exposed to air. Notice that the Raman spectrum of the 2-month-old restacked film, Fig. 6(b), is almost the same as that of the original $2H\text{-MoS}_2$ powder, Fig. 6(c). In such films x-ray diffraction shows that the original crystal spacing between the layers is recovered.² The conversion back to the trigonal prism coordination is likely related to a recovery of the sulfur-sulfur interaction between the single molecular layers on the expulsion of water.

From Figs. 5(b) and 5(c) it is also evident that the J_1 , J_2 , and J_3 peaks persist, with significant intensity, in the spectra obtained from the aged samples. This occurs despite the fact that the coordination of the Mo atoms appear to be changing to the $\tau\text{-MoS}_2$ form, as evidenced by the increasing intensity of the 383-cm^{-1} mode. These observations suggest, most probably, that both the τ and Ω phases are present in the sample. The effects of aging were simulated by thermally annealing some restacked films at 300°C for one hour. There was no significant difference between the Raman spectra of the annealed

films and the spectra of films that were aged at room temperature for 2 months.

IV. CONCLUSIONS

A valence-force-field model has been applied to a study of the lattice dynamics of MoS_2 single molecular layers. Symmetry considerations and a lattice-dynamical calculation both indicate that the strong 383-cm^{-1} Raman mode that is present in spectra obtained from crystalline $2H\text{-MoS}_2$ should also be Raman active in single-layer trigonal-prism-coordinated $\tau\text{-MoS}_2$ but inactive in single-layer octahedrally coordinated $\Omega\text{-MoS}_2$. The absence of this mode in our spectra thus indicates that the single layers of MoS_2 are octahedrally coordinated as suggested by x-ray diffraction experiments.² If the suspensions of single layers of MoS_2 are allowed to age over days and weeks the 383-cm^{-1} mode reappears and becomes stronger with age. It is postulated that this apparent gradual transition to the $\tau\text{-MoS}_2$ phase results from a restacking of some of the layers within the suspension. This structural conversion appears to occur much more rapidly in restacked films of single layers of MoS_2 , presumably as a result of the much more rapid evaporation of the water that surrounds the individual layers.

The Raman spectra obtained from single layers of MoS_2 also contain strong features at 156 (J_1), 226 (J_2), and 333 (J_3) cm^{-1} which are absent, in spectra obtained^{5,6} from $2H\text{-MoS}_2$. The presence of these features is attributed to a zone-folding mechanism which results from the formation² of a superlattice in the basal planes of the single layers of MoS_2 . If the layers are assumed to possess a distorted octahedral structure,¹⁷ similar to that of WTe_2 , a $2a_0 \times a_0$ basal plane superlattice would result and the three peaks should arise from phonons at the M point being folded into the center of the new Brillouin zone. A lattice-dynamics model appropriate to a distorted octahedral structure yielded values for M -point frequencies of $\Omega\text{-MoS}_2$ which are in good agreement with the observed frequencies of J_1 , J_2 , and J_3 . The line shapes of the observed features are qualitatively consistent^{21,22} with the nature of the appropriate dispersion curves and a crystallite basal plane dimension of about 50 \AA . We thus conclude that the single layers of MoS_2 possess a distorted octahedral structure. As the single molecular layers restack with the expulsion of water and the sulfur-sulfur intralayer interaction is recovered, their structure converts back to the trigonal prismatic coordination of crystalline $2H\text{-MoS}_2$.

ACKNOWLEDGMENT

The financial support of the Natural Sciences and Engineering Research Council of Canada is gratefully acknowledged.

- *On leave from Departamento de Física, Centro de Investigación y de Estudios Avanzados del Instituto Politécnico Nacional, Apartado Postal 14-740, 07000 México, Distrito Federal, México.
- ¹P. Joensen, R. F. Frindt, and S. R. Morrison, *Mater. Res. Bull.* **21**, 457 (1986).
- ²D. Yang, S. Jiménez-Sandoval, W. M. R. Divigalpitiya, J. C. Irwin, and R. F. Frindt, *Phys. Rev. B* **43**, 12 053 (1991).
- ³J. L. Verble and T. J. Wieting, *Phys. Rev. Lett.* **25**, 362 (1970).
- ⁴J. L. Verble and T. J. Wieting, *Solid State Commun.* **11**, 941 (1972).
- ⁵C. S. Wang and J. M. Chen, *Solid State Commun.* **14**, 1145 (1974).
- ⁶J. M. Chen and C. S. Wang, *Solid State Commun.* **14**, 857 (1974).
- ⁷O. P. Agnihotri, H. K. Sehgal, and A. K. Garg, *Solid State Commun.* **12**, 135 (1973).
- ⁸T. J. Wieting and J. L. Verble, *Phys. Rev. B* **3**, 4286 (1971).
- ⁹G. Lucovsky, R. M. White, J. A. Benda, and J. F. Revelli, *Phys. Rev. B* **7**, 3859 (1973).
- ¹⁰N. Wakabayashi, H. G. Smith, and R. M. Nicklow, *Phys. Rev. B* **12**, 659 (1975).
- ¹¹R. A. Bromley, *Philos. Mag.* **23**, 1417 (1971).
- ¹²T. J. Wieting and J. L. Verble, in *Electrons and Phonons in Layered Crystal Structures*, edited by T. J. Wieting and M. Schlüter (Reidel, Dordrecht, Holland, 1979). The paper on MoS₂ is T. J. Wieting, *Solid State Commun.* **12**, 931 (1973).
- ¹³M. Plishke, K. K. Bardhan, R. Leonelli, and J. C. Irwin, *Can. J. Phys.* **61**, 397 (1983).
- ¹⁴W. M. R. Divigalpitiya, S. R. Morrison, and R. F. Frindt, *Thin Solid Films* **186**, 177 (1990).
- ¹⁵X. R. Qin, D. Yang, R. F. Frindt, and J. C. Irwin, unpublished.
- ¹⁶P. Joensen, E. D. Crozier, N. Alberding, and R. F. Frindt, *J. Phys. C* **20**, 4043 (1987).
- ¹⁷W. G. Dawson and D. W. Bullett, *J. Phys. C* **20**, 6159 (1987).
- ¹⁸B. E. Brown, *Acta Crystallogr.* **20**, 268 (1966).
- ¹⁹J. L. Feldman, *Phys. Rev. B* **25**, 7132 (1982).
- ²⁰R. Shuker and R. W. Gammon, *Phys. Rev. Lett.* **25**, 222 (1970).
- ²¹H. Richter, Z. P. Wang, and L. Ley, *Solid State Commun.* **39**, 625 (1981).
- ²²I. H. Campbell and P. M. Fauchet, *Solid State Commun.* **58**, 739 (1986).
- ²³K. K. Tiong, P. M. Amiritharaj, F. H. Pollak, and D. E. Aspnes, *Appl. Phys. Lett.* **44**, 122 (1984).
- ²⁴R. S. Berg, N. Mavalvala, and T. Steinberg, *IEEE J. Elect. Mat.* **19**, 1323 (1990).
- ²⁵A. S. Barker and A. J. Sievers, *Rev. Mod. Phys.* **47**, 51 (1975).
- ²⁶R. J. Nemanich and S. A. Solin, *Phys. Rev. B* **20**, 392 (1979).
- ²⁷See, for example, L. J. Raubenheimer and G. Gilat, *Phys. Rev.* **157**, 586 (1967).